Structural and Magnetization Studies of a New (μ-Oxo)bis(μ-carboxylato)dimanganese(III) Complex with a Terminal Hydroxo Ligand

Montserrat Corbella,* Ramon Costa, and Joan Ribas

Departament de Química Inorgànica, Universitat de Barcelona, Diagonal, 647, 08028-Barcelona, Spain

Pascal H. Fries,* Jean-Marc Latour, and Lars Öhrström

CEA/Département de Recherche Fondamentale sur la Matière Condensée, Laboratoire SESAM/CC (URA CNRS 1194), Centre d'Etudes Nucléaires de Grenoble. 38054-Grenoble Cedex 9, France

Xavier Solans and Víctor Rodríguez

Departament de Cristal.lografia i Dipòsits Minerals, Universitat de Barcelona, Martí i Franquès, s/n, 08028-Barcelona, Spain

Received July 27, 1995[⊗]

The dinuclear Mn^{III} complex $[Mn_2O(PhCOO)_2(bpy)_2(OH)(NO_3)]\cdot H_2O$ was prepared by controlled oxidation of manganous nitrate with *n*-tetrabutylammonium permanganate in the presence of benzoic acid (PhCOOH) and 2,2′-bipyridine (bpy). Its structure was determined in a single-crystal X-ray diffraction experiment, and consists of a triply-bridged $[Mn_2(\mu\text{-O})(\mu\text{-PhCOO})_2]^{2+}$ dinuclear core. Each manganese(III) ion bears a chelating bpy and a terminal X anion ($X = OH^-$ or NO_3^-) completing a distorded octahedral coordination geometry. Although the terminal anions are located in disordered positions, the analysis of bond lengths and steric considerations led us to assign to the complex an asymmetric structure $[(bpy)(OH)Mn^{III}(\mu\text{-O})(\mu\text{-PhCOO})_2Mn^{III}(bpy)(ONO_2)]$. The product, with a chemical formula $C_{34}H_{29}Mn_2N_5O_{10}$, crystallizes in the monoclinic system, space group $C2/c$, with $a = 16.607(4)$ Å, $b = 25.619(6)$ Å, $c = 9.796(3)$ Å, $\beta = 100.15(3)°$, and $Z = 4$. Magnetic studies performed on a series of related compounds have revealed a moderate ferro- or antiferromagnetic interaction and significant zero-field splittings in line with the strong Jahn−Teller distortion of the high spin d^4 manganese(III) ions. In the present work we interpreted the magnetic properties of the complex using a spin Hamiltonian which includes the Heisenberg exchange, axial and rhombic ZFS, and an anisotropic Landé factor, under the assumption of a pseudo-C_2 symmetry of the dinuclear core. In order to determine the anisotropy parameters with enough accuracy, we resorted to variable-temperature variable-field magnetization measurements over the 2−300 K range at fields of 0.5, 1.0, 2.5, and 5 T. The whole set of data was fit with a single set of parameters through diagonalization of the complete spin Hamiltonian. The best fit values $J = +1.0(4)$ cm^{-1}, $D = +4.5(5)$ cm^{-1}, $E = 0$, $g_x = g_y = 1.96$, and $g_z = 2.00$ showed that a ferromagnetic interaction occurs between manganese(III) ions in a compressed octahedral environment. A magnetostructural relationship linking the ferromagnetic behavior of the dinuclear complex to the compression of the Mn(III) coordination sphere (and conversely of the antiferromagnetism to the elongation) is then proposed. It is substantiated by theoretical molecular orbital calculations of the extended Hückel type.

Introduction

In the past two decades manganese has been implicated as an essential cofactor of various enzymatic systems where it can be either an enzyme activator or an essential part of the active site.[1−4] In the latter case various nuclearities have been observed from mononuclear sites as in superoxide dismutase[5] to the tetranuclear site of oxygen evolution in photosystem II.[6] Nevertheless, a growing number of manganese proteins have been shown to possess a dinuclear active site.[7] Some of them are understood to operate at the $Mn^{II}Mn^{II}$ level,[1,7] but in others the function involves a change in the oxidation state of the pair. Manganese catalase[8] is the prototype of these enzymes. The first evidence that it contains a dimanganese unit came from electronic absorption spectroscopy, which showed a spectrum typical of the (μ-oxo)(μ-carboxylato)dimanganese(III) cores.[8a] Its active site has been shown to exist under several redox forms $Mn^{II}Mn^{II}$, $Mn^{II}Mn^{III}$, $Mn^{III}Mn^{III}$, and $Mn^{III}Mn^{IV}$.[8b] A low resolution X-ray structure determination of the oxidized Mn^{III}-Mn^{III} protein from *Thermus thermopilus* has revealed that the two metal ions are 3.6 Å apart.[8c] On the other hand, EXAFS

[⊗] Abstract published in *Advance ACS Abstracts,* February 15, 1996.

(1) Wieghardt, K. *Angew. Chem., Int. Ed. Engl.* **1989**, *28*, 1153.
(2) Que, L.; True, A. E. *Prog. Inorg. Chem.* **1990**, *38*, 97.
(3) (a) Vincent, J. B.; Christou, G. *Adv. Inorg. Chem.* **1989**, *33*, 197. (b) Christou, G. *Acc. Chem. Res.* **1989**, *22*, 328.
(4) Pecoraro, V. L., Ed. *Manganese Redox Enzymes*; VCH Publishers: New York, 1992.
(5) (a) Stallings, W. C.; Pattridge, K. A.; Strong, R. K.; Ludwig, M. *J. Biol. Chem.* **1985**, *260*, 16424. (b) Parker, M. W.; Blake, C. F. *J. Mol. Biol.* **1988**, *199*, 649.
(6) Thorp, H. H.; Brudvig, G. W. *New J. Chem.* **1991**, *15*, 479.
(7) Reczkowski, R. S.; Ash, D. E. *J. Am. Chem. Soc.* **1992**, *114*, 10992.
(8) (a) Kono, Y.; Fridovich, I. *J. Biol. Chem.* **1983**, *258*, 6015. (b) Waldo, G. S.; Yu, S.; Penner-Hahn, J. E. *J. Am. Chem. Soc.* **1992**, *112*, 5869. (c) Barynin, V. V.; Vagin, A. A.; Melik-Adamyan, V. R.; Grebenko, A. I.; Khangulov, S.; Popov, A. N.; Andrianova, M. E.; Vainshtein, B. K. *Dokl. Akad. Nauk SSSR* **1986**, *288*, 877. (d) Khangulov, S. V.; Voyevodskaya, N. V.; Barynin, V. V.; Grebenko, A. I.; Melik-Adamyan, V. R. *Biofizika* **1987**, *32*, 960. (e) Fronko, R. M.; Penner-Hahn, J. E.; Bender, C. J. *J. Am. Chem. Soc.* **1988**, *110*, 7554.

0020-1669/96/1335-1857$12.00/0

experiments have evaluated to 2.67 Å the intermetallic distance in the superoxidized form $Mn^{III}Mn^{IV}$ of the protein from *Lactobacillus plantarum*.[8d,e] Moreover, the binuclear nature of the catalase active site has been supported by the observation of a 16-line EPR spectrum probably associated with the mixed-valence $Mn^{III}Mn^{IV}$ form of proteins from *T.* thermopilus[8b] as well as from *L.* plantarum.[8e] This observation suggests that the active site structure of manganese catalase is similar to those observed for the binuclear non heme iron proteins hemerythrin[9] and ribonucleotide reductase.[10] In fact, the substitution of iron by manganese(II) has been performed in the latter protein from *Escherichia coli*, and an intermanganese distance of 3.6 Å has been determined by X-ray crystallography, supporting this analogy.[11] In line with these results are the observations of manganese counterparts of the iron enzymes ribonucleotide reductase[12] and purple acid phosphatases[13] although the latter case is controversial.[14]

Modeling the spectroscopic properties and the reactivity of manganese catalase and of the manganese cluster in PS II is of major interest to inorganic chemists. This has led to the isolation of polynuclear manganese complexes in various oxidation states and their structural and magnetic characterization.[1−4] However, only a few of them exhibited the (μ-oxo)(μ-carboxylato)-dimanganese(III) unit[15,16] present at the catalase active site and postulated as a component of the tetranuclear cluster in PS II. Two kinds of compounds with this core have been obtained: (i) The use of a tetraammine ligands furnishes (μ-oxo)(μ-carboxylato) dimanganese(III) hexacoordinate complexes.[17] (ii) Tridentate capping ligands lead to hexacoordinate complexes with a (μ-oxo)bis(μ-carboxylato)dimanganese(III) core.[18] On the other hand, the use of bidentate ligands such as bipyridine also give rise to dinuclear complexes of (μ-oxo)bis(μ-carboxylato)dimanganese(III) core where the coordination of each manganese ion is saturated by an easily exchangeable ligand such as a water molecule or an anion (chloride, azide), which might allow some reactivity.[19]

We report the isolation and structural characterization through X-ray crystallography of a (μ-oxo)bis(μ-carboxylato)dimanganese(III) complex which bears a hydroxide and a nitrate ion at terminal coordination sites. The magnetic behavior of the compound has been studied. To account simultaneously for the exchange interaction, the zero-field effects and *g* anisotropy, a multifield magnetization study was performed and the data were analyzed through full diagonalization of the total Hamiltonian using an improved numerical procedure. Such a complete analysis has never been reported for complexes of this kind.[20] In this procedure the four sets of data obtained through temperature variations over the range 2−300 K at fields of 0.5, 1, 2.5, and 5 T were fitted simultaneously using a single set of parameters.

Experimental Section

Synthesis. ***Caution!*** Appropriate care should be exercised in the use of $Bu^n_4NMnO_4$. All manipulations were performed under aerobic conditions with materials as received. $Bu^n_4NMnO_4$ was prepared as described.[21]

To obtain the compound $[Mn_2O(PhCOO)_2(bpy)_2(OH)(ONO_2)]\cdot H_2O$ (**1**), solid bpy (0.5 g, 3.2 mmol) was added to a stirred solution of $Mn(NO_3)_2\cdot 4H_2O$ (0.64 g, 2.5 mmol) and benzoic acid (0.24 g; 2 mmol) in MeCN (100 mL). The resulting yellow solution was treated with an acetonitrile solution of $Bu^n_4NMnO_4$ (0.23 g, 0.7 mmol). After a few minutes, a dark green microcrystalline precipitate of **1** deposited. The solid was collected by filtration, washed with MeCN, and dried. A solution of **1** was left to evaporate slowly in order to obtain X-ray quality crystals. The yield of the reaction was *ca.* 70%. Anal. Calcd for $C_{34}H_{29}Mn_2N_5O_{10}$: C, 52.52; H, 3.76; N, 9.01. Found: C, 52.3; H, 3.6; N, 9.2. IR (KBr, cm^{-1}): 3390 (s, br), 1598 (s), 1558 (s), 1495 (w), 1470 (m), 1448 (s), 1384 (vs), 1310 (w), 1250 (w), 1175 (w), 1160 (w), 1105 (w), 1070 (w), 1060 (w), 1035 (m), 1023 (m), 840 (w), 828 (m), 769 (s), 728 (s), 720 (s), 680 (w), 662 (w), 653 (w).

IR and Magnetic Measurements. Infrared spectrum (4000−400 cm^{-1}) was recorded from a KBr pellet in a NICOLET 520 FT-IR spectrometer. Magnetization measurements were performed on an MPMS SQUID magnetometer operating at four fields (0.5, 1, 2.5, and 5 T) over the temperature range 2−300 K. The polycrystalline sample (36.13 mg) was contained in a Kel-F bucket which had been calibrated at the same fields and temperatures. The diamagnetic correction was calculated using Pascal's constants.[22]

X-ray Crystallography. A prismatic crystal of **1** (0.1 × 0.1 × 0.2 mm) was selected and mounted on an Enraf-Nonius CAD4 four-circle diffractometer. Unit cell parameters were determined from automatic centring of 25 reflections ($12 < \theta < 21°$) and refined by the least-squares method. Intensities were collected with graphite monochromatized MoKα radiation, using $\omega/2\theta$ scan technique. A total of 3102 reflections were measured in the range $1.5 < \theta < 25$, 2373 of which were assumed as observed applying the condition $I > 2\sigma(I)$. Three reflections were measured every 2 h as orientation and intensity control; significant intensity decay was not observed. Corrections were made for Lorentz−polarization but not for absorption.

Crystallographic parameters and details of the data collection and reduction are given in Table 1 and in Supporting Information. The structure was solved by Patterson synthesis, using the SHELXS computer program[23] and refined by the full-matrix least-squares method, with the SHELX93 computer program[24] using 3052 reflections (very negative intensities were not taken into account). The function

(9) Stenkamp, R. E.; Sieker, L. E.; Jensen, L. H. *J. Am. Chem. Soc.* **1984**, *106*, 618.
(10) Nordlund, P.; Sjöberg, B. M.; Eklund, H. *Nature* **1990**, *345*, 593.
(11) Atta, M.; Nordlund, P.; Åberg, A.; Eklund, H.; Fontecave, M. *J. Biol. Chem.* **1992**, *267*, 20682.
(12) Willing, A.; Follman, H.; Auling, G. *Eur. J. Biochem.* **1988**, *170*, 603.
(13) Fujimoto, S.; Murakami, K.; Ohara, A. *J. Biochem.* **1985**, *97*, 1777.
(14) Hefler, S. K.; Averill, B. A. *Biochem. Biophys. Res. Commun.* **1987**, *146*, 1173.
(15) Wieghardt, K. *Angew. Chem. Int. Ed. Engl.* **1989**, *28*, 1153.
(16) (a) Vincent, J. B.; Christou, G. *Adv. Inorg. Chem.* **1989**, *33*, 197. (b) Christou, G. *Acc. Chem. Res.* **1989**, *22*, 328.
(17) (a) Oberhausen, K. J.; O'Brien, R. J.; Richardson, J. F.; Buchanan, R. M.; Costa, R.; Latour, J. M.; Tsai, H. L.; Hendrickson, D. N. *Inorg. Chem.* **1993**, *32*, 4561. (b) Arulasmy, N.; Glerup, J.; Hazell, A.; Hodgson, D. J.; McKenzie, C. J.; Toftlund, H. *Inorg. Chem.* **1994**, *33*, 3023.
(18) (a) Wieghardt, K.; Bossek, U.; Ventur, D.; Weiss, J. *J. Chem. Soc. Chem. Comm.* **1985**, 347. (b) Wieghardt, K.; Bossek, U.; Bonvoisin, J.; Beauvillain, P.; Girerd, J. J.; Nuber, B.; Weiss, J.; Henzo, J. *Angew. Chem. Int. Ed. Engl.* **1986**, *25*, 1030. (c) Sheats, J. E.; Czernuszewicz, R. S.; Dismukes, G. C.; Rheingold, A. L.; Petrouleas, V.; Stubbe, J.; Armstrong, W. H.; Beer, R. H.; Lippard, S. J. *J. Am. Chem. Soc.* **1987**, *109*, 1435. (d) Wieghardt, K.; Bossek, U.; Nuber, B.; Weiss, J.; Bonvoisin, J.; Corbella, M.; Vitols, S. E.; Girerd, J. J. *J. Am. Chem. Soc.* **1988**, *110*, 7398. (e) Wu, F. J.; Kurtz, D. M.; Hagen, K. S.; Nyman, P. D.; Debrunner, P. G.; Vankai, V. A. *Inorg. Chem.* **1990**, *29*, 5174. (f) Mahapatra, S.; Lal, T. K.; Mukherjee, R. *Inorg. Chem.* **1994**, *33*, 1579.
(19) (a) Ménage, S.; Girerd, J. J.; Gleizes, A. *J. Chem. Soc., Chem. Commun.* **1988**, 431. (b) Vincent, J. B.; Folting, K.; Huffman, J. C.; Christou, G. *Biochem. Soc. Trans.* **1988**, *16*, 822. (c) Blackman, A. G.; Huffman, J. C.; Lobkovsky, E. B.; Christou, G. *J. Chem. Soc., Chem. Commun.* **1991**, 989. (d) Vincent, J. B.; Tsai, H. L.; Blackman, A. G.; Wang, S.; Boyd, P. D. W.; Folting, K.; Huffman, J. C.; Lobkovsky, E. B.; Hendrickson, D. N.; Christou, G. *J. Am. Chem. Soc.* **1993**, *115*, 12353.
(20) (a) Day, Holm et al. have performed a similar analysis but without taking into account the anisotropy of the *g* factor, in spite of the fact that fitting of the magnetization data resulted in a *g* value departing from 2. (b) Yu, S. B.; Wang, C. P.; Day, E. P.; Holm, R. H. *Inorg. Chem.* **1991**, *30*, 4067.
(21) (a) Sala, T.; Sargent, M. V. *J. Chem. Soc., Chem. Commun.* **1978**, 253. (b) Vincent, J. B.; Folting, K.; Huffman, J. C.; Christou, G. *Inorg. Chem.* **1986**, *25*, 996.
(22) Mabbs, F. E.; Machin, D. J. *Magnetism and Transition Metal Complexes*; Chapman and Hall Ltd.: London, 1973; p 5.
(23) Sheldrick, G. M.; *Acta Cryst.*, **1990**, *A46*, 467.
(24) Sheldrick, G. M. SHELXL, A Programme for Crystal Structure Refinement. University of Göttingen, Germany, 1994.

Table 1. Crystallographic Data for $[Mn_2O(PhCOO)_2(bpy)_2(OH)(ONO_2)]\cdot H_2O$ (**1**)

chem formula: $C_{34}H_{29}Mn_2N_5O_{10}$	fw = 777.51
a, Å = 16.607(4)	space group:[a] $C2/c$ (No. 15)
b, Å = 25.619(6)	T = 20(2) °C
c, Å = 9.796(3)	λ(Mo Kα) = 0.710 69 Å
α = 90.0°	ρ_{calcd}, = 1.260 g/cm^3
β = 100.15(3)°	μ(Mo Kα) = 6.70 cm^{-1}
γ = 90.0°	R^b = 0.0346
V = 4102.5(10) Å^3	$R_w{}^c$ = 0.0930
Z = 4	

[a] Hahn, T., Ed. *International Tables for Crystallography*; Kluwer Academic Publications: Dordrecht, The Netherlands. 1992; Vol. A. [b] $R = \sum||F_o| - |F_c||/\sum|F_c|$. [c] $R_w = (\sum w(||F_o|^2 - |F_c|)^2/\sum w|F_c|^2)$.

minimized was $\sum w||F_o|^2 - |F_c|^2|^2$, where $w = [\sigma^2(I) + (0.1497P)^2]^{-1}$, and $P = (|F_o|^2 + 2|F_c|^2)/3$; f, f' and f'' were taken from ref 25. The extinction coefficient was 0.00007(13). The final R (on F) factor was 0.034, R_w (on $|F|^2$) = 0.093, and goodness-of-fit = 0.554 for all observed reflections. The number of refined parameters was 270. Maximum shift/esd = 0.093, mean shift/esd = 0.06, maximum and minimum peaks in the final difference synthesis were +0.406 and −0.212 e Å^{-3}, respectively.

Some special features of the structure determination are summarized as follows. The use of the space group $C2/c$ to refine the structure led the ligands NO_3 and OH and the water molecule of crystallization to be located in disorder positions. Attempts at refining the crystal structure in space group Cc resulted in the localization of the nitrato and hydroxo ligands on each manganese atom of the dinuclear unit. Nevertheless, this causes the elements of the covariance matrix to approach unity, which hampers the convergence of the structure refinement. This result may be attributed to the fact that most of the electronic density in the dinuclear entity is related by a 2-fold axis, while the possible nonequivalent atoms represent only 10% of the F(000) value. Therefore, the former space group was assumed: we should consider the use of the $C2/c$ group as a tool to refine the structure, which gives us an accurate description of the dinuclear unit with the exception of the atoms not related by the 2-fold axis.

Occupancy factors for NO_3 and OH were assumed at 0.5, while that for H_2O was refined, obtaining the values of 0.21(3) for O(W) and 0.29(3) for O(W′). 13 hydrogen atoms were computed and refined with an overall isotropic temperature factor using a riding model (these positions are given in Table S5). The disorder of the nitrato and hydroxo ligands led us to consider the possibility of both $O_2NO-Mn-O-Mn-ONO_2$ and $HO-Mn-O-Mn-OH$ units disordered in the crystal cell. However, this possibility was rejected, because two adjacent bis(nitrato) units would give O(5)−O(5)(ii) and O(6)−O(6)(ii) distances of 1.132 and 1.022 Å respectively, resulting in very strong steric hindrance.

Finally, we must distinguish which of the coordinating oxygen atoms, O(7) or O(4), belongs to either the nitrato or the hydroxo ligands. The typical $Mn-O-NO_2$ angle when a nitrate anion acts as a terminal ligand fell within the 115−130° range. If we assign O(7) as pertaining to the NO_3^- group, the calculated angle is 129.7°, in agreement with that expected. O(4), which gives a value of 138.9°, was then considered as the OH oxygen atom.

Final atomic coordinates are listed in Table 2. Complete listings of final positional parameters, bond lengths and angles, anisotropic thermal parameters and calculated hydrogen coordinates are given in Tables S2 to S5 (Supporting Information) respectively.

Computational Details. All the extended Hückel molecular orbital calculations and drawings were performed on an IBM 486DX2 Personal Computer with the CACAO[26] package, v4.0. The extended Hückel calculation program is a major revision of the original program SIMCON (Cornell University) and uses the weighted Wolfsberg−Helmholz formula[27] for the nondiagonal elements of the matrix H. The atomic parameters were taken from the literature.[28−30]

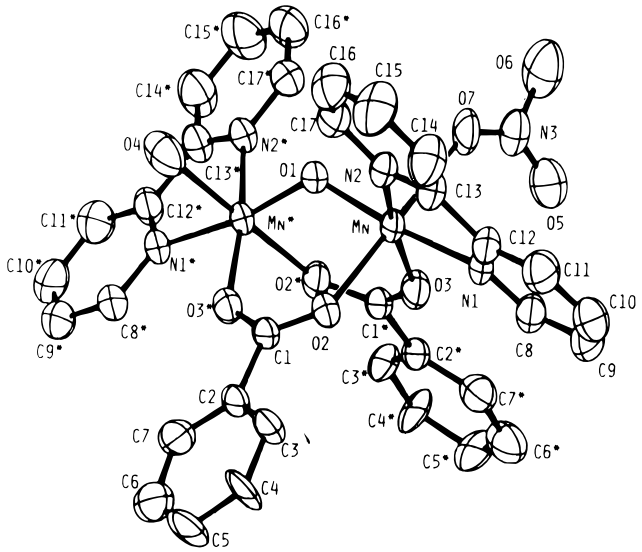

Figure 1. Molecular structure and atom labelling scheme of $[Mn_2O(PhCOO)_2(bpy)_2(OH)(NO_3)]H_2O$.

Table 2. Atomic Coordinates ($\times 10^4$) and Equivalent Isotropic Displacement Parameters ($\times 10^3$) for $C_{34}H_{29}Mn_2N_5O_{10}$ (**1**)

	x/a	y/b	z/c	U_{eq},[a] Å^2
Mn	5683(1)	6846(1)	1576(1)	61(1)
O(1)	5000	7171(1)	2500	65(1)
O(2)	6124(1)	6319(1)	3259(2)	75(1)
O(3)	4945(1)	6299(1)	659(2)	79(1)
O(4)	5324(13)	7386(7)	−101(17)	122(6)
N(1)	6628(1)	6590(1)	627(2)	71(1)
N(2)	6629(1)	7348(1)	2390(2)	69(1)
C(1)	5754(2)	6149(1)	4152(2)	62(1)
C(2)	6155(2)	5725(1)	5095(2)	67(1)
C(3)	6958(2)	5602(1)	5078(2)	81(1)
C(4)	7323(2)	5200(1)	5891(3)	107(1)
C(5)	6910(3)	4918(1)	6683(3)	113(1)
C(6)	6117(3)	5040(1)	6720(3)	117(1)
C(7)	5715(2)	5450(1)	5928(3)	88(1)
C(8)	6563(2)	6217(1)	−326(3)	93(1)
C(9)	7235(2)	6054(1)	−880(4)	106(1)
C(10)	7934(3)	6269(2)	−451(4)	115(1)
C(11)	8040(2)	6657(1)	532(4)	103(1)
C(12)	7361(2)	6814(1)	1047(3)	73(1)
C(13)	7355(2)	7242(1)	2043(2)	76(1)
C(14)	8045(2)	7531(2)	2601(4)	114(1)
C(15)	7970(3)	7926(2)	3485(4)	133(1)
C(16)	7213(3)	8042(2)	3789(4)	113(1)
C(17)	6564(2)	7740(1)	3237(3)	86(1)
N(3)	5125(3)	7380(3)	−1274(5)	88(1)
O(5)	5050(4)	6986(3)	−1914(5)	125(2)
O(6)	4967(4)	7803(3)	−1991(4)	145(2)
O(7)	5358(10)	7441(7)	−166(13)	98(4)
OW	4972(9)	8369(6)	508(25)	134(7)
OW′	4472(50)	8528(17)	−169(59)	285(36)

[a] U_{eq} is defined as one-third of the trace of the orthogonalized $\mathbf{U}_{ij}$ tensor: $U_{eq} = {}^1/_3\ \mathrm{Tr}[\sum \mathbf{U}_{ij} a_i^* a_j^*]$.

Results and Discussion

Description of the Structure. Figure 1 illustrates the structure of the complex. It consists of a neutral dinuclear unit

(25) *International Tables for X-ray Crystallography*; Kynoch Press: Birminghan, England, 1974; Vol. IV, pp 99, 100, and 149.
(26) Mealli, C.; Proserpio, D. M. Computer Aided Composition of Atomic Orbitals: A package of Programs for Molecular Orbital Analysis. PC Version 4.0, 1994. Original Reference: Mealli, C.; Proserpio, D. M. *J. Chem. Educ.* **1990**, *67*, 399. Revisions made by: Linn, K.; Sironi, A.; Lopez, J. A.
(27) Ammeter, J. H.; Bürgi, H. B.; Thibeault, J. C.; Hoffmann, R. *J. Am. Chem. Soc.* **1978**, *100*, 3686.
(28) Hoffmann, R. *J. Chem. Phys.* **1963**, *39*, 1397.
(29) Summerville, R. H.; Hoffmann, R. *J. Am. Chem. Soc.* **1976**, *98*, 7240.
(30) Alvarez, S. *Tables of Parameters for Extended Hückel Calculations*; Universitat de Barcelona: Barcelona, Spain, 1992.

Table 3. Selected Bond Lengths[a] (Å) and Angles[a] (deg) for $C_{34}H_{29}Mn_2N_5O_{10}$ (**1**)

Mn−O(1)	1.7774(10)	Mn−Mn(i)	3.1405(6)
Mn−O(2)	2.158(2)	O(2)−C(1)	1.234(3)
Mn−O(3)	1.971(2)	O(3)−C(1)(i)	1.267(3)
Mn−O(4)	2.15(2)	N(3)−O(5)	1.181(7)
Mn−O(7)	2.28(2)	N(3)−O(6)	1.293(7)
Mn−N(1)	2.068(2)	N(3)−O(7)	1.10(2)
Mn−N(2)	2.077(2)		
Mn(i)−O(1)−Mn	124.12(11)	N(1)−Mn−O(2)	87.82(7)
O(1)−Mn−O(3)	99.48(7)	N(2)−Mn−O(2)	87.83(7)
O(1)−Mn−N(1)	168.75(7)	O(4)−Mn−O(2)	176.3(6)
O(3)−Mn−N(1)	91.64(7)	O(1)−Mn−O(7)	88.8(3)
O(1)−Mn−N(2)	91.26(7)	O(3)−Mn−O(7)	95.0(4)
O(3)−Mn−N(2)	169.18(8)	N(1)−Mn−O(7)	88.5(3)
N(1)−Mn−N(2)	77.67(8)	N(2)−Mn−O(7)	86.4(4)
O(1)−Mn−O(4)	88.4(5)	O(2)−Mn−O(7)	173.7(4)
O(3)−Mn−O(4)	92.5(6)	N(3)−O(7)−Mn	129.7(12)
N(1)−Mn−O(4)	89.5(5)	O(2)−C(1)−O(3)(i)	125.6(2)
N(2)−Mn−O(4)	89.1(6)	C(1)−O(2)−Mn	128.1(2)
O(1)−Mn−O(2)	93.79(6)	C(1)(i)−O(3)−Mn	131.31(14)
O(3)−Mn−O(2)	90.17(7)		

[a] Symmetry transformation used to generate equivalent atoms: (i) $-x+1, y, -z+{}^1/_2$.

with two benzoates and an oxide ion bridging the two manganese ions. Each manganese is chelated by a bipyridine, and the coordination sphere is completed by different oxygen anions: a nitrate and a hydroxide. The latter is hydrogen bonded to a water molecule of crystallization. Selected bond distances and angles are collected in Table 3.

Owing to the impossibility of locating the hydrogen atoms on the terminal hydroxo ligand, there is an uncertainty between a hydroxide and a water molecule, corresponding respectively to either a $(OH)Mn^{III}Mn^{III}$ or a $(H_2O)Mn^{II}Mn^{III}$ formula. The hydroxo−dimanganese(III) formulation was based on the following considerations : (i) the Mn−O distance (2.15 Å) is significantly shorter than the corresponding manganese-nitrate bond ($Mn-ONO_2 = 2.28$ Å) and than the $Mn-OH_2$ distances (*ca.* 2.30 Å) found in aqua complexes;[19a,d] (ii) magnetic data support the $Mn^{III}Mn^{III}$ formulation (see below).

With the exception of the hydroxo and nitrato ligands, all the remaining atoms are related by a 2-fold axis perpendicular to the line joining the Mn(III)−Mn(III) cations and passing through the bridging oxo anion.

The manganese ions exhibit very distorded octahedral geometries, which are characteristic of high spin d^4 Mn^{III} ions undergoing a strong Jahn−Teller distortion, showing significant rhombicity in both sites (see below). There are two sets of Mn−O(carboxylate) distances of 1.971 and 2.158 Å. The first set corresponds to the O(3) atoms in *trans* position with respect to the bipyridine nitrogen N(2). The carboxylate C(1)−O(3) associated distance is 1.267 Å, indicating a mostly single bond character. The longer second group occupies the *trans* position to the hydroxide and nitrate anions, and is compensated by a shorter C(1)−O(2) bond distance of 1.234 Å, corresponding to a predominantly double bond character.

Magnetic Properties. The magnetic properties of the complex are illustrated, in Figure 2, as the temperature dependence of the product of the molar susceptibility by the temperature. At 300 K, $\chi_M T$ amounts to 6 cm^3 K mol^{-1}, which is the value expected for two independent spins $S = 2$. When the temperature decreases, the $\chi_M T$ product increases slightly: this behavior is characteristic of a system exhibiting a ferromagnetic interaction. A maximum value of about 7 cm^3 K mol^{-1} is reached in the range of 10−30 K, depending on the strength of the applied field. This value is far below the one expected for a system of spin $S = 4$ ($\chi_M T = 10$ cm^3 K mol^{-1}).

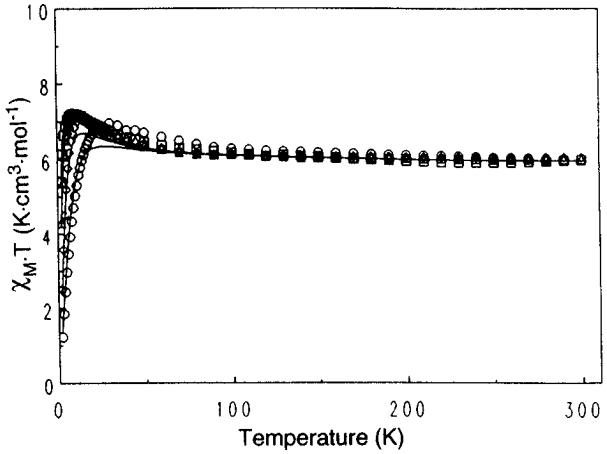

Figure 2. Temperature dependence of the χT product at 0.5 (□), 1 (△), 2.5 (◇), and 5 (○) T.

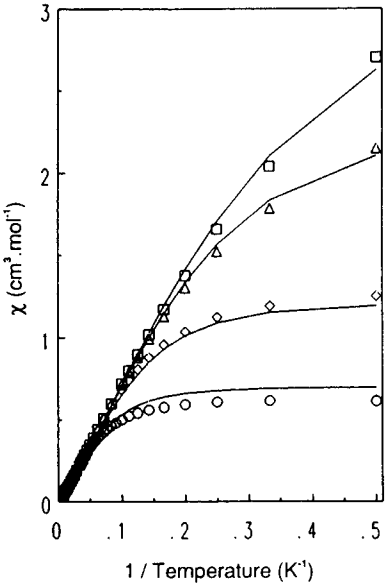

Figure 3. Variation of the molar susceptibility (χ) witht the inverse of the temperature at 0.5 (□), 1 (△), 2.5 (◇), and 5 (○) T.

At lower temperatures ($T < 10$ K), a steep decrease in $\chi_M T$ is observed, which is strongly dependent on the field strength. The latter feature appears in Figure 3, which presents the dependence of the molar susceptibility on the inverse of the temperature at different fields. This behavior is characteristic of the occurence of significant zero field splittings in the Mn(III) ions.

Theoretical Analysis of the Magnetic Data. In line with the high spin d^4 electronic configuration of the ions the magnetic properties of manganese(III) complexes are dominated at low temperatures by axial zero-field splitting effects of a few wavenumbers.[31] As noted by Hendrickson,[17] axial zero-field splitting parameters cannot be determined accurately by fitting bulk magnetic susceptibility data. In addition, Mn^{III} complexes are strongly affected by Jahn−Teller distorsions.[19] Both effects give rise to large anisotropy of the Lande factor *g*. On the other hand, magnetic susceptibility studies of the (μ-oxo)(μ-carboxylato)dimanganese(III) complexes have shown that the two ions undergo a weak magnetic exchange interaction ($H = -2J\mathbf{S}_a\cdot\mathbf{S}_b$) in the range $-5 < J < 10$ cm^{-1}. Accordingly, the zero-field splitting and the exchange interaction are of comparable magnitude, which precludes the use of a perturbational treatment of the spin Hamiltonian.

(31) (a) Behere, D. V.; Mitra, S. *Inorg. Chem.* **1980**, *19*, 992. (b) Kennedy, B. J.; Murray, K. S. *Inorg. Chem.* **1985**, *24*, 1552.

In order not to increase the number of parameters, the two Mn(III) ions, Mn* and Mn, are assumed to be located in symmetry related coordination environments a and b respectively, taking into account the existence of a pseudo-C_2 axis. So, their fine structure Hamiltonians H_{fs}(a) and H_{fs}(b), and their Zeeman **g** tensors **g**(a) and **g**(b), are assumed to be identical with respect to symmetric direct reference frames (O_a, $\hat{i}_a$, $\hat{j}_a$, $\hat{k}_a$) and (O_b, $\hat{i}_b$, $\hat{j}_b$, $\hat{k}_b$) associated with the a and b sites. The centers O_a and O_b of the frames are taken to be the Mn(III) centers. The unit vectors $\hat{k}_a$, $\hat{k}_b$ lie along the vectors joining the Mn(III) ions to the bridging oxygen O1, which is bound to both Mn(III) ions. The unit vectors $\hat{i}_a$ and $\hat{i}_b$ should be orthogonal to the vectors $\hat{k}_a$ and $\hat{k}_b$, respectively. They are defined as the following normalized vector products:

$$\hat{i}_a = \frac{\overrightarrow{\text{Mn(a),O3*}} \times \hat{k}_a}{||\overrightarrow{\text{Mn(a),O3*}} \times \hat{k}_a||}$$

$$\hat{i}_b = \frac{\overrightarrow{\text{Mn(b),O3}} \times \hat{k}_b}{||\overrightarrow{\text{Mn(b),O3}} \times \hat{k}_b||}$$

where $\overrightarrow{\text{Mn(a),O3*}}$ and $\overrightarrow{\text{Mn(b),O3}}$ are the vectors joining the Mn(a) ion to the bonding oxygen O3*, and the Mn(b) ion to the bonding oxygen O3, respectively. Finally, we define the unit vectors $\hat{j}_a = \hat{k}_a \times \hat{i}_a$ and $\hat{j}_b = \hat{k}_b \times \hat{i}_b$, which lie on the planes O1, Mn(a), O3* and O1, Mn(b), O3 respectively.

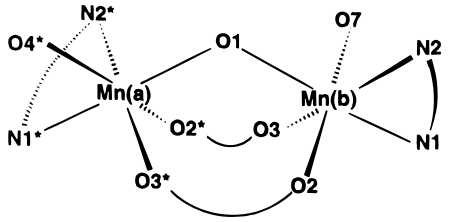

For each site, denoting the spin of the Mn(III) cation by $\mathbf{S}_i$, the single-ion Hamiltonian is defined as:[32]

$$H(i) = H_{fs}(i) + H_Z(i) \quad (1a)$$

The fine structure part H_{fs}(i) is restricted to the terms of the second degree in $S_{i\alpha}$ ($\alpha = x, y, z$). In the site reference frame (O_i, $\hat{i}_i$, $\hat{j}_i$, $\hat{k}_i$) it is given by

$$H_{fs}(i) = d[S_{ix}^2 - {}^1/_3 S_i(S_i + 1)] + E[S_{ix}^2 - S_{iy}^2] \quad (1b)$$

D and E being the axial and rhombic parameters of the zero-field splitting (ZFS) tensors. The anisotropic Zeeman interaction is

$$H_z(i) = \mu_B (g_x H_{ix} S_{ix} + g_y H_{iy} S_{iy} + g_z H_{iz} S_{iz}) \quad (1c)$$

where H_{ix}, H_{iy}, H_{iz} are the components of the external field **H** in the site reference frame. The simplifying hypothesis is made that, for each magnetic ion, the ZFS tensor and the Zeeman **g** factor can be diagonalized simultaneously. Now, the two Mn(III) spins are assumed to be coupled by an isotropic exchange interaction J. The total spin Hamiltonian of the dimer reads:

$$H_{tot} = H(b) - 2J\mathbf{S}_a \cdot \mathbf{S}_b \quad (2)$$

In order to diagonalize H_{tot} the site Hamiltonian should be expressed with respect to the same reference molecular frame (O, $\hat{i}$, $\hat{j}$, $\hat{k}$). Let $R(i) = [R(i)_{\alpha\beta}]$ ($\alpha, \beta = 1, 2, 3$) be the rotation which transforms the unit vectors of the molecular frame to those of the site reference frame (O_i, $\hat{i}_i$, $\hat{j}_i$, $\hat{k}_i$). The fine structure Hamiltonians can be rewritten in terms of second-rank irreductible tensor of operators[33] $\mathbf{T}(S_i)_{2q}$. For any spin **S** these operators are defined as:[34]

$$\mathbf{T}(S)_{20} = \frac{N_2}{\sqrt{6}}[3S_z^2 - S(S+1)]$$

$$\mathbf{T}(S)_{2\pm1} = \mp\frac{N_2}{2}[(S_xS_z + S_zS_x) \pm i(S_yS_z + S_zS_y)] \quad (3)$$

$$\mathbf{T}(S)_{2\pm2} = \frac{N_2}{2}[S_x^2 - S_y^2 \pm i(S_xS_y + S_yS_x)]$$

where

$$N_2 = \left[\frac{30}{(2S+3)(2S+1)S(2S-1)(S+1)}\right]^{1/2}$$

The fine structure Hamiltonians become:

$$H_{fs}(i) = \sum_{q=-2}^{2} f_q \mathbf{T}(S_i)_{2q} \quad (4a)$$

with

$$f_0 = \frac{\sqrt{6}}{3N_2}D,\ f_{\pm1} = 0,\ \text{and}\ f_{\pm2} = \frac{E}{N_2} \quad (4b)$$

Let $R^{(2)}_{qp}(i)$ ($q, p = -2, ..., +2$) be the coefficients of the Wigner rotation matrix of order 2 associated with the active rotation[33] $R(i) = [R(i)_{\alpha\beta}]$. The rotation property of the tensor operator is

$$\mathbf{T}(S_i)_{2p} = \sum_{q=-2}^{2} \mathbf{T}(S_i)^{mol}_{2q} R^{(2)}_{qp}(i) \quad (5)$$

where the $\mathbf{T}(S_i)_{2q}{}^{mol}$ are the tensor operators which are built with the spin components in the molecular reference frame according to eq 3. Using eqs 4 and 5, the fine structure Hamiltonians can be rewritten in the molecular reference frame as

$$H_{fs}(i) = \sum_{q=-2}^{2}\left[\sum_{p=-2}^{2} R^{(2)}_{qp}(i)\, f_p\right]\mathbf{T}(S_i)_{2q}{}^{mol} \quad (6)$$

Similarly, the Zeeman Hamiltonians in the molecular frame become

$$H_Z(i) = \mu_B \sum_{\alpha,\beta = x,y,z} g_{\alpha\beta}{}^{mol}(i)\, H_\alpha S_{i\beta} \quad (7a)$$

where the H_α are the components of the external magnetic field

(32) Abragam, A.; Bleaney, B. *Electron Paramagnetic Resonance of Transition Ions*; Dover Publications: New York, 1970; p 133.

(33) Messiah, A. *Mécanique Quantique*; Dunod: Paris, 1972; Vol. 2, p 447.

(34) Blum, K. *Density Matrix Theory and Applications*; Plenum Press: London, 1981; p 85.

in the molecular axes and where the **g** factors are

$$g_{\alpha\beta}^{\text{mol}}(\text{i}) = \sum_{\alpha'=x,y,z} R(\text{i})_{\alpha\alpha'} R(\text{i})_{\beta\alpha'} g_{\alpha'} \qquad (7b)$$

To sum up, the total spin Hamiltonian in the molecular reference frame, H_{tot}, is defined by eq 2, where the fine structure and Zeeman parts of the single-ion Hamiltonians are given by eqs 6 and 7, respectively.

The average molar magnetization $M_a(H)$ along the direction of the magnetic field **H** is calculated numerically. It is given by

$$M_A(H) = N_{\text{Avog}} \frac{1}{4\pi} \int_0^{\pi} \sin\theta \, d\theta \int_0^{2\pi} [h\hat{\mathbf{u}}(\theta,\phi)] \, dm_{||} \quad (8a)$$

where $m_{||}$ is the dimer magnetization parallel to the field and θ, ϕ are the spherical coordinates, with respect to the dimer molecular reference frame, of the unit vector $\hat{\mathbf{u}}(\theta,\phi)$, which points in the field direction. The dimer magnetization is calculated as the numerical derivative

$$m_{||} = -\frac{\partial}{\partial H} F \, [H \, \hat{u}(\theta, \phi)] \qquad (8b)$$

of the free energy[35]

$$F \, [H\hat{\mathbf{u}}(\theta,\phi)] = -k_B T \ln\left\{\sum_n \exp\left[-\frac{E_n \, [H\hat{\mathbf{u}}(\theta,\phi)]}{k_B T}\right]\right\} \quad (8c)$$

where the E_n are the energy levels of the total spin Hamiltonian for the magnetic field $H \, \hat{\mathbf{u}}(\theta,\phi)$. The energy spectrum of H_{tot} is invariant under time reversal[32] so that $F(-H) = F(H)$, and

$$m_{||}[H\hat{\mathbf{u}}(\theta,\phi)] = m_{||}[H\hat{\mathbf{u}}((\pi - \theta),(\phi + \pi))] \qquad (9)$$

The simulation of the experimental data was conducted through a least-squares fit for all the magnetic fields with the six parameters, J, D, E, g_x, g_y, and g_z, of the dimer Hamiltonian, defined by eqs 2, 6, and 7. For each set of parameters the double integral in (8a) is computed by the Cartesian product of six-point Gauss integration formulas[36,37] over θ and ϕ. The quadrature over ϕ is reduced to the $[0,\pi]$ interval because of the symmetry relation in (9); this explains why six tabulation points are sufficient for the Gauss quadrature over ϕ. This numerical procedure minimizes the number of field directions θ, ϕ for which the magnetizations $m_{||}$ are computed[38] from the energy levels E_n obtained by rather lengthy numerical diagonalizations of the 25×25 matrices of the dimer Hamiltonian H_{tot}.

It was assumed that both manganese ions have identical Zeeman **g** tensors and zero-field splittings. Moreover, the influence of rhombicity was considered specifically. Preliminary calculations revealed that E and the difference between g_x and g_y did not significantly affect the results and could not be accurately estimated. Accordingly, the final calculations were performed with the following set of parameters: $g_x = g_y$, g_z, J, D, and $E = 0$. When all four independent parameters are allowed to vary, the final values of J and D were always positive with $J < D$, but the g values showed a strong tendency to depart from 2: g_z up to *ca.* 2.3 and $g_x = g_y$ down to 1.7. Neither value is physically meaningful, and therefore the range of variation was restricted to 1.95−2.00. Owing to the fact that the g factors are most sensitive to the high temperature data while J and D values are more important in the low temperature domain, we performed the simulation in two successive phases, first using the $\chi_M T$ products, which slightly overvalue the high temperature data, to obtain precise estimation of the g factors. Then we fixed these values in simulations of the molar susceptibilities χ_M, a procedure which overvalues the low temperature data where J and D can be accurately determined. Such a procedure gave a satisfactory fit of the experimental data with the following set of parameters: $J = +1.0(4)$ cm^{-1}, $D = +4.5(5)$ cm^{-1}, $g_x = g_y = 1.96$, and $g_z = 2.00$.

Discussion of the Magnetic Properties. The correlation between magnetic and structural properties of dinuclear complexes has attracted much interest in the past twenty years from both the experimental and the theoretical standpoints.[39−41] In particular, Hoffmann[41] has studied the influence of the d orbital electron count on the bending of the M−O−M angle in the μ-oxo metalloprotein dimers. These works have shown that the leading interactions are the ones involving the d_{z^2}, d_{xz}, and d_{yz} orbitals on each metal: d_{z^2}–d_{z^2}, d_{xz}−d_{xz}, and d_{yz}−d_{yz}. A similar analysis allowed Holm[42] to explain the geometrical preferences of μ-oxo and μ-sulfido diferric complexes.

In the past decade, numerous magnetostructural studies have been devoted to μ-oxo−μ-carboxylato dinuclear complexes of titanium to copper in the first transition series, as well as selected ions of the second and third ones. In the case of (μ-oxo)(μ-carboxylato)diferric complexes, Que[43] has shown that no dependence of the exchange interaction on the Fe−O−Fe angle can be observed. On the other hand, Gorun and Lippard[44] have found, for an extensive series of similar complexes, an empirical correlation between the exchange integral and the Fe-(μ-O) distance. The d_{z^2}–d_{z^2} interaction has been perceived as the most important one leading to an antiferromagnetic interaction. Accordingly, it has been proposed that the depopulation of the d_{z^2} orbitals and the resulting cancellation of their interaction was responsible for the drastic lessening of the antiferromagnetic exchange on going from Fe(III) to Mn(III) compounds. This view has been challenged in a recent article by Wieghardt and Girerd,[45] who present a qualitative rationalization of the differences observed in the exchange interactions with the occupation of the metal d orbitals. In particular, they have stressed the importance of the so-called "crossed interactions" involving orbitals of different kinds on each metal. From Extended Hückel calculations they have shown that for systems with M−O−M angles around 120° the d_{yz}−d_{yz} and d_{xz}−d_{z^2} interactions are as important as the d_{z^2}–d_{z^2} one. In Fe^{III}−O−Fe^{III} derivatives the three interactions are antiferromagnetic, resulting in strong antiferromagnetic exchange ($J = ca. -100$ cm^{-1}). In the case of (μ-oxo)dimanganese(III) complexes, where the d_{z^2} orbital is vacant, the d_{z^2}–d_{z^2} interaction vanishes and the d_{xz}−d_{z^2} ones, which involve mixing of a singly occupied

(35) Ashcroft, N. W.; Mermin, N. D. *Solid State Physics*; Saunders: Philadelphia, PA, 1976; p 643.
(36) Johnson, L. W.; Riess, R. D. *Numerical Analysis*; Addison-Wesley: London, 1982; p 324.
(37) Stroud, A. H. *Mathematical Methods for Digital Computers*; Wiley: London, 1967; Vol. II, p 145.
(38) We have written a Fortran program AN2G (*an*isotropic hamiltonian for *2 g*eneral spins) of about 2500 statements long following this procedure.
(39) Hay, P. J.; Thibeault, J. C.; Hoffmann, R. *J. Am. Chem. Soc.* **1978**, *97*, 3686.
(40) Kahn, O.; Charlot, M. F. *Nouv. J. Chim.* **1980**, *4*, 567.
(41) Tatsumi, K.; Hoffmann, R. *J. Am. Chem. Soc.* **1981**, *103*, 3328.
(42) Mukherjee, R. N.; Stack, T. D. P.; Holm, R. H. *J. Am. Chem. Soc.* **1988**, *110*, 1681.
(43) Norman, R. E.; Holz, R. C.; Ménage, S.; Que, L.; Zhang, J. H.; O'Connor, C. J. *Inorg. Chem.* **1990**, *29*, 4629.
(44) Gorun, S. M.; Lippard, S. J. *Inorg. Chem.* **1991**, *7*, 1625.
(45) R. Hotzelmann, R.; Wieghardt, K.; Flörke, U.; Haupt, H. J.; Weatherburn, D. C.; Bonvoisin, J.; Blondin, G.; Girerd, J. J. *J. Am. Chem. Soc.* **1992**, *114*, 1681.

Table 4. Magnetostructural Correlations between the Crystallographic Parameters of the $[Mn^{III}_2(\mu\text{-O})(\mu\text{-O}_2CR)_2]^{2+}$ Core and the Spin Hamiltonian Constants for Some Structurally Characterized Dinuclear Complexes

complex	J, cm^{-1}	D, cm^{-1}	structural params[a]	distortion	ref
(A) $[Mn_2(\mu\text{-O})(\mu\text{-AcO})_2(Me_3TACN)_2](ClO_4)_2$	+9	+3	3.94/4.28/4.28 0.34; 0	compression	18a,d
(B) $[Mn_2(\mu\text{-O})(\mu\text{-AcO})_2(HB(pz)_3)_2]\cdot 4CH_3CN$	<-0.2[b,c]	*c*	3.84/4.21/4.27 0.37; 0.06	compression	18c
(C) $[Mn_2(\mu\text{-O})(\mu\text{-O}_2CPh)_2(N_3)_2(bpy)_2]$	+8.8[b]	+0.3	3.89/4.18/4.25 0.29; 0.07	compression	19d
(D) $[Mn_2(\mu\text{-O})(\mu\text{-O}_2CPh)_2(OH)(NO_3)(bpy)_2]$	+1	+4.5	3.85/4.05/4.3−4.4 0.20; 0.25−0.35	rhombic	*d*
(E) $[Mn_2(\mu\text{-O})(\mu\text{-AcO})_2(TMIP)_2](ClO_4)_2$	<-0.2[b,c]	*c*	3.85/4.05/4.3−4.4 0.20; 0.25−0.35	rhombic	18e
(F) $[Mn_2(\mu\text{-O})(\mu\text{-AcO})_2(H_2O)_2(bpy)_2](ClO_4)_2$	−3.4[b]	*c*	3.87/4.01/4.46 0.13; 0.45	elongation	19d
(G) $[Mn_2(\mu\text{-O})(\mu\text{-AcO})_2(Cl)_2(bpy)_2]$	−4.1[b]	−0.07	3.87/4.02/4.7−4.8 0.15; 0.7−0.8	elongation	19d

[a] Upper line: averaged sums of the bond distances for opposite equivalent ligands in the Mn(III) coordination spheres. The first one corresponds to the Mn−(μ-O) bonds and their respective trans ligands. Lower line: difference between each pair of parameters. [b] The J values reported have been converted to the Heisenberg Hamiltonian convention used in this work: $-2JS_1S_2$. [c] The spin Hamiltonian employed does not take into acount the anisotropy. For very weak magnetic exchange interactions, this may cause a fictitious antiferromagnetic behavior. [d] Present work.

orbital (d_{xz}) with an empty one (d_{z^2}), are ferromagnetic. The importance of such contributions is inversely proportional to the energy difference of the two orbitals involved. These interactions compete with the $d_{yz}-d_{yz}$, which is still antiferromagnetic, and as a consequence, the overall exchange is weakly ferro- or antiferromagnetic, depending on subtle structural and electronic factors. This analysis falls short of explaining the change in the sign of the exchange coupling in the series of dimanganese(III) complexes which has been extended since its publication.

In the (μ-oxo)bis(μ-carboxylato)dimanganese(III) bis(bipyridine) complexes, the magnetic exchange switches from antiferromagnetic in the chloro and aquo derivatives to ferromagnetic in the azido one. To explain this difference, Hendrickson[19d] relies on the influence of the exogeneous ligand on the $d_{x^2-y^2}$ orbital: in the case of the azido ligand, which is a stronger ligand (Mn−N 2.122 Å), the energy of the orbital is higher and its antiferromagnetic contribution through a pathway involving the carboxylates is smaller than for the weaker chloro (average Mn−Cl 2.56 Å) and aquo (average Mn−O 2.285 Å) ligands. Since the hydroxo (Mn−O 2.15 Å) and nitrato (Mn−O 2.28 Å) terminal ligands are rather strongly bound, this interpretation holds for the present compound also.

However, as stated above, the structural properties of high-spin manganese(III) complexes are dominated by the occurence of strong Jahn−Teller distortions. This feature has not been taken into account to explain the magnetic properties of manganese(III) dimers and, as detailed below, it can provide the basis to rationalize the structural and magnetic data of all compounds in this series. Manganese(III) ions can experience two types of distortions of their octahedral surroundings: either a compression, when the distances on one axis are considerably shorter than the ones on the other two directions, or an elongation, where the distances on one axis are longer. These structural differences translate into different electronic configurations: a $^5A_1$ ground state with a configuration $(d_{xy})^1(d_{xz})^1(d_{yz})^1(d_{x^2-y^2})^1$ is associated to a compressed ion, while an elongated one possesses a $(d_{xz})^1(d_{yz})^1(d_{xy})^1(d_{z^2})^1$ configuration with a $^5B_1$ ground state. Gerritsen and Sabinsky[46] have shown that the magnetic properties of a Mn(III) ion depend on the type of distortion: for example, the sign of the axial ZFS parameter D is positive for a compression and negative for an elongation. In both descriptions, the distortions are taken along the z axis, and the x and y axis point toward the equatorial ligands. It is worth noting that the theoretical study of Wieghardt and Girerd[45] was done for the case of compressed ions.

One can argue that the type of distortion of the Mn(III) ion which dictates the occupancy of the d_{z^2} orbital will decide the sign of the magnetic exchange through its contributions as detailed by Girerd[45] (see above). However, the actual situation is more complicated. Table 4 lists the structural and magnetic properties of the seven (μ-oxo)bis(μ-carboxylato)dimanganese(III) compounds for which both studies have been performed. The structural properties are given in the form of the averaged sums of the bond distances for opposite equivalent ligands of both Mn(III) ions in the complex. The differences between two successive indexes are also given. Examination of the data shows that (i) the two types of first-order Jahn−Teller distortion are observed in these compounds and (ii) the axis of the distortion changes—for the compression it goes through the bridging oxide while the elongation axis passes through a carboxylate oxygen and the exogenous ligand; (iii) more rhombicity is associated to an elongation of the coordination sphere; (iv) Table 4 reveals a correlation between a ferromagnetic interaction and a compression of the manganese coordination octahedron.

Owing to the change of distortion axis, the orbital description of the problem is not straightforward and extended Hückel molecular orbital calculations have been undertaken to investigate the orbital interactions susceptible to mediate the magnetic exchange.

Molecular Orbital Calculations. Extended Hückel molecular orbital calculations were performed along the approach outlined by Wieghardt and Girerd.[45] These authors assumed that the bridging ligand most important to mediate the magnetic interactions is the oxo group, since the metal−oxide bond distances are the shortest. The carboxylato bridges contribute to a far lesser extent as shown experimentally. Accordingly, we did not take them into account explicitly, and in the calculations they were replaced by hydroxo groups.

Calculations were then performed on two model dinuclear isomers $[(NH_3)_3(OH)_2Mn(\mu\text{-O})Mn(OH)_2(NH_3)_3]$, representing the two limiting structural situations: compression and elongation of the octahedral geometry. For both isomers, we fixed the geometry parameters which do not vary significantly in the series depicted in Table 4: the Mn−(μ-O) and Mn−(N−trans-μ-O) distances were set to 1.80 and 2.10 Å respectively and the Mn−(μ-O)−Mn angle was fixed to 120°. Finally, the coordination geometries around the Mn atoms were kept strictly

(46) Gerritsen, H. J.; Sabinsky, E. S. *Phys. Rev.* **1963**, *132*, 1507.

octahedral, with 90° angles between ligands, in order to simplify the study of these systems. The geometry parameters for the hydroxo ligands were an O−H distance of 1.00 Å and an Mn−O−H angle of 109°. In the NH_3 groups we set a N−H distance of 1.03 Å and H−N−H angles of 109°.

For the compressed dinuclear complexes related in Table 4, it is found experimentally that the four Mn−O(carboxylate) distances are similar, as the corresponding Mn−N(trans-carboxylate) distances do. A C_{2v} point symmetry was then imposed on the model compound by using the following parameters: Mn−OH distances of 2.00 Å and Mn−(N−cis-μ-O) distances of 2.10 Å.

In the elongated isomer, the values were Mn−(OH1) = 2.20 Å and Mn−(N−trans-OH1) = 2.30 Å for the elongation axis and Mn−(OH2) = 1.90 Å and Mn−(N−trans-OH2) = 2.10 Å for the short one. It is important to realize that in this case a C_2 symmetry results, according to the fact that each carboxylate ligand has two different Mn−O bond lengths.

The distortion axes found in these systems are

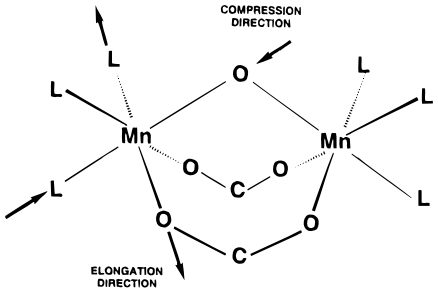

In the first case, compression of the octahedral geometry occurs along the local axis bearing the oxo group. The five d orbitals of each metallic fragment are in decreasing order of energies: d_{z^2}, $d_{x^2-y^2}$, (d_{xz}, d_{yz}), and d_{xy}, as expected for an axially compressed octahedron. When the two fragments approach to form the dinuclear complex, the local symmetry axes (z) coincide with the Mn−(μ-O) bonds. As a consequence, the metal contribution of the magnetic orbitals are essentially identical with the ones of the mononuclear fragment except for the fact that the degenerate pairs (d_{xz}, d_{yz}) mix through the σ_v symmetry plane to give the two symmetry-adapted combinations D_A and D_B. The latter orbitals are displayed in Figure 4 and can be deduced from the original (d_{xz}, d_{yz}) orbitals by a 45° rotation. At this stage, four superexchange interactions involving the oxo bridge can be identified: three direct interactions d_{z^2}–d_{z^2}, D_A-D_A, and D_B-D_B and a crossed interaction $D_A-d_{z^2}$. The intensity of the D_B-D_B interaction is strong and independent of the Mn−(μ-O)−Mn angle, but for values close to 120° the D_A-D_A interaction is weak. Since both orbitals are occupied in high-spin Mn(III) ions, these two interactions are antiferromagnetic in nature. On the other hand, the vacancy of the d_{z^2} orbital cancels the d_{z^2}–d_{z^2} interaction and makes the strong $D_A-d_{z^2}$ interaction ferromagnetic. To sum this up, two leading interactions are operative in the compressed dinuclear complex: the direct interaction D_B-D_B, which is antiferromagnetic, and the crossed interaction $D_A-d_{z^2}$, which is ferromagnetic. This explains why the corresponding complexes can exhibit weak ferromagnetic couplings. This analysis is quite in line with Girerd's findings.

In the elongated complexes the shortest bonds are again the Mn−(μ-O) ones and the elongation axis is along one Mn−carboxylate direction. As a consequence, the two Mn−carboxylate axes are no longer equivalent and the symmetry of the dinuclear complexes is lowered from C_{2v} to C_2: the Mn(III) ions are now in a rhombically distorded octahedral

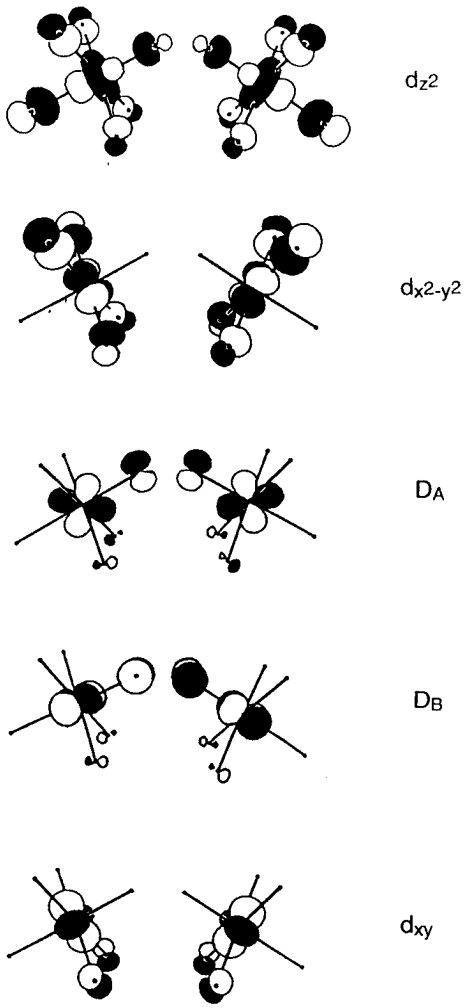

Figure 4. Magnetic orbitals of the mononuclear fragments of the $[Mn_2O(OH)_4(NH_3)_6]$ complex in the case of a compressed Jahn−Teller distortion.

geometry. The analysis of the symmetry adapted magnetic orbitals of the fragments is more complicated than in the previous case. Due to the descent in symmetry, the three low-lying d orbitals mix together to form three symmetry adapted combinations D_1, D_2, and D_3 (see Figure 5). The lobes of these orbitals do not lie any more either on the axes or in the planes of the coordination octahedron. On the contrary, the orbitals are distorted and tilted in such a way that all of them include a contribution from the oxo p orbitals. Therefore, all interactions must be taken into account. When compared to the compressed case it is seen that the two main interactions D_2-D_2 (antiferromagnetic and analogous to D_B-D_B) and $D_1-(d_{x^2-y^2})$ (ferromagnetic as $D_A-d_{z^2}$) are conserved, but additional interactions are now operative. In particular, significant crossed interactions between D_1 on one manganese and d_{z^2} on the other are now allowed and they are antiferromagnetic in nature. The number of antiferromagnetic pathways of exchange is thus increased in the elongated geometry over the compressed one, which explains the overall antiferromagnetic couplings observed for these complexes.

Summary and Conclusions

In this article we have described the structural and magnetic properties of an asymmetric dimanganese(III) complex. Multifield saturation magnetization studies have been used to obtain both the exchange coupling and the zero field splittings of the

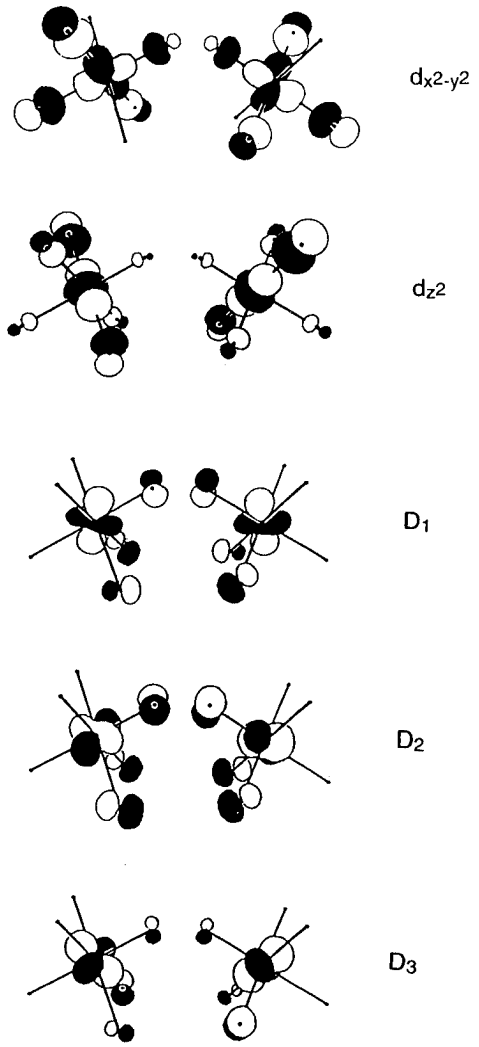

Figure 5. Magnetic orbitals of the mononuclear fragments of the $[Mn_2O(OH)_4(NH_3)_6]$ complex in the case of an elongated Jahn−Teller distortion.

ions. This has been done through full diagonalization of the corresponding Hamiltonian including the anisotropy of the *g* factor.

Positive values have been derived for *J* and *D* parameters. The same relationship between the sign of the exchange and the sign of the axial zero-field splitting of the Mn(III) ions is found for all known complexes with the same core. This observation leads us to propose that the Jahn−Teller distortions of the Mn(III) ions play a crucial role in the magnetic properties of the (μ-oxo)bis(μ-carboxylato) dimanganese(III) species. This hypothesis is supported by EH-MO calculations, which show that switching the distortion of the octahedral Mn(III) site from compression to elongation along a carboxylate bond lowers the symmetry of the system and activates additional interactions of antiferromagnetic nature in the dinuclear compound. As a consequence, an overall antiferromagnetic exchange is observed in the elongated systems while compressed ones are ferromagnetically coupled.

When comparing the bipyridine complexes with exogenous ligands (compounds C, F, and G in Table 4), it appears that these ligands dictate the behavior of the complex. Actually, ligands such as chloro (average Mn−Cl: 2.55 Å) and aqua (average Mn−OH_2: 2.28 Å) form long bonds that produce elongated Mn sites which couple antiferromagnetically. On the other hand, the strongly binding azido ligand (average Mn−N: 2.12 Å) gives compressed Mn sites which favor a ferromagnetic interaction.

The dinuclear complex we have reported (compound D in Table 4) contains a strongly binding hydroxo (Mn−OH: 2.15 Å) and a weakly binding nitrato (Mn−ONO_2: 2.28 Å) ligands, what corresponds to an intermediate situation. In this complex the effect of the hydroxide appears to dominate, since the complex exhibits the characteristic features of the compressed case: a weak ferromagnetic coupling, a positive ZFS parameter and the relationship $g_{\|} = 2.0 > g_{\perp}$[47] in accordance to an octahedral coordination of the Mn(III) ion better described as compressed.

Acknowledgment. Stimulating discussions with Dr. J. J. Girerd are acknowledged. L.Ö. thanks the Wenner-Gren Center Foundation for Scientific Research for a post-doctoral fellowship. M.C., R.C., and J.R. are grateful for financial assistance from the DGICYT through Project PB93/0772.

Supporting Information Available: Tables giving details of the structure determination and crystal data, atom coordinates, bond lengths, bond angles, anisotropic thermal parameters, and hydrogen atom coordinates (6 pages). Ordering information is given on any current masthead page.

IC950930X

(47) Abragam, A.; Bleaney, B. *Electron Paramagnetic Resonance of Transition Ions*; Dover Publications: New York, 1970; p 434.